Journal of Neuroscience Research 86:326–338 (2008)

Peptide Hormone Exendin-4 Stimulates Subventricular Zone Neurogenesis in the Adult Rodent Brain and Induces Recovery in an Animal Model of Parkinson's Disease

Göran Bertilsson, Cesare Patrone, Olof Zachrisson, Annica Andersson, Karin Dannaeus, Jessica Heidrich, Jarkko Kortesmaa, Alex Mercer, Elisabet Nielsen, Harriet Rönnholm, and Lilian Wikström*

NeuroNova AB, Stockholm, Sweden

We investigated the effects of exendin-4 on neural stem/progenitor cells in the subventricular zone of the adult rodent brain and its functional effects in an animal model of Parkinson's disease. Our results showed expression of GLP-1 receptor mRNA or protein in the subventricular zone and cultured neural stem/progenitor cells isolated from this region. In vitro, exendin-4 increased the number of neural stem/progenitor cells, and the number of cells expressing the neuronal markers microtubule-associated protein 2, β-III-tubulin, and neuron-specific enolase. When exendin-4 was given intraperitoneally to naïve rodents together with bromodeoxyuridine, a marker for DNA synthesis, both the number of bromodeoxyuridine-positive cells and the number of neuronal precursor cells expressing doublecortin were increased. Exendin-4 was tested in the 6-hydroxydopamine model of Parkinson's disease to investigate its possible functional effects in an animal model with neuronal loss. After unilateral lesion and a 5-week stabilization period, the rats were treated for 3 weeks with exendin-4. We found a reduction of amphetamine-induced rotations in animals receiving exendin-4 that persisted for several weeks after drug administration had been terminated. Histological analysis showed that exendin-4 significantly increased the number of both tyrosine hydroxylase- and vesicular monoamine transporter 2-positive neurons in the substantia nigra. In conclusion, our results show that exendin-4 is able to promote adult neurogenesis in vitro and in vivo, normalize dopamine imbalance, and increase the number of cells positive for markers of dopaminergic neurons in the substantia nigra in a model of Parkinson's disease.

Key words: adult neural stem cells; differentiation; GLP-1; 6-hydroxydopamine

In the adult mammalian brain, new neurons and glial cells are continuously generated from a proliferating population of neural progenitor/stem cells (NSC) that become incorporated into the existing brain by a process known as adult neurogenesis (Emsley et al., 2005). This process occurs mainly in the subventricular zone (SVZ)/olfactory bulb and hippocampal dentate gyrus (Gage et al., 1995; Emsley et al., 2005). The existence of active, functional adult neurogenesis raises the possibility that pharmacological stimulation of endogenous neural stem/progenitor cells could lead to cell regeneration that may be beneficial in central nervous system disorders where cell loss occurs, e.g., Parkinson's disease (PD), stroke, and Alzheimer's disease (Emsley et al., 2005; Taupin, 2006).

The peptide hormone exendin-4 was originally isolated from the saliva of the lizard *Heloderma suspectum* (gila monster; Eng et al., 1992) and is a potent and selective agonist for the GLP-1 receptor (GLP-1R; Goke et al., 1993; Thorens et al., 1993; Wheeler et al., 1993). Exendin-4 is used clinically to treat diabetes type II and displays glucoregulatory effects, including glucose-dependent enhancement of insulin secretion (Goke et al., 1993; Greig et al., 1999; Parkes et al., 2001; Egan et al., 2002) and glucose-dependent suppression of high glucagon secretion (Kolterman et al., 2003). Because of its longer plasma half-life, exendin-4 is preferred over the endogenous mammalian GLP-1R ligand, GLP-1, which is rapidly degraded (Kieffer et al., 1995). Exendin-4 also enhances liver glycogen storage (Knauf et al., 2005) and slows gastric emptying (Kolterman et al., 2003). Intriguingly, intact exendin-4 has the ability to pass the blood–brain barrier in mouse (Kastin and Akerstrom, 2003) and can exert central nervous system

The first two authors contributed equally to this work.

*Correspondence to: Lilian Wikström, NeuroNova AB, Fiskartorpsvägen 15 A-D, S-114 33 Stockholm, Sweden.
E-mail: lilian.wikstrom@neuronova.com

Received 21 December 2006; Revised 26 June 2007; Accepted 26 June 2007

Published online 5 September 2007 in Wiley InterScience (www.interscience.wiley.com). DOI: 10.1002/jnr.21483

(CNS) effects (Calvo et al., 1995; Goke et al., 1995; Merchenthaler et al., 1999). CNS effects of exendin-4 have been shown by direct, intracerebroventricular (i.c.v.) administration to promote neurotrophic or neuroprotective actions (Perry et al., 2003). In addition, specific GLP-1R stimulation can enhance cognitive functions in rodents (During et al., 2003). Earlier in vitro studies have shown that exendin-4 can promote neurite outgrowth in PC12 cells (Perry et al., 2002); protect cultured hippocampal neurons from apoptotic insult (Perry et al., 2003); and stimulate transcription of tyrosine hydoxylase (TH), the rate-limiting enzyme for the dopamine (DA) synthesis, in brainstem catecholamine neurons (Yamamoto et al., 2002). Because of the pleiotropic effects of exendin-4 in the CNS, we set out to investigate whether this peptide was able to modulate neurogenesis and functional recovery after neuronal loss in the adult brain.

Our results show that exendin-4 stimulates adult neurogenesis in vitro and in vivo. In addition to these findings, we also provide evidence that exendin-4 has the ability to restore function in a 6-hydroxydopamine (6-OHDA) animal model of PD. Finally, our results show that exendin-4 treatment results in an increase in the number of neurons positive for TH and vesicular monoamine transporter 2 (VMAT2) in the substantia nigra (SN) of animals lesioned with 6-OHDA compared with untreated, lesioned control.

MATERIALS AND METHODS

Reagents

Exendin-4 (E-7144), rat serum albumin (RSA), Tween, Triton X-100, hyaluronidase, fast diaminobenzidine (DAB), microtubule-associated protein 2 (MAP-2) antibody, H_2O_2, DAPI, DNase, trypsin, and trypsin/EDTA in Hank's balanced salt solution (HBSS) were from Sigma-Aldrich (St. Louis, MO). Dulbecco's modified Eagle's medium (DMEM), DMEM/F12, DMEM + glutamax-I, fetal calf serum (FCS), B27 supplement, penicillin, streptomycin, basic fibroblast growth factor (bFGF), N2 supplement, and trypsin/EDTA were from Invitrogen (La Jolla, CA). GLP-1 (7–37) was from Phoenix Pharmaceuticals. Epidermal growth factor (EGF) was from BD Biosciences (San Jose, CA). The doublecortin (DCX) antibody was from Santa Cruz Biotechnology (Santa Cruz, CA) and the Vectastain ABC kit from Vector Laboratories (Burlingame, CA). Xylene-based mounting medium was from Richard Allan Scientific. The β-III-tubulin antibody was from BioSite and neuron-specific enolase (NSE) antibody from Polysciences Inc. (Warrington, PA). The GLP-1R detection antibody (ab1318) was from Abcam and the biotinylated secondary antibody (BA-1000) from Vector Laboratories. The mouse anti-DCX antibody, TH (AB152), and VMAT2 (AB1767) were from Chemicon (Temecula, CA). The rat monoclonal anti-BrdU antibody was from Harlan and Hoechst 33342 from Molecular Probes (Eugene, OR). DNase I was from Ambion (Austin, TX) and paraformaldehyde from Merck.

Cell Culture

The anterior wall of the lateral ventricle of 5-week-old mice (C57 black) was enzymatically dissociated in 0.8 mg/ml hyaluronidase and 0.5 mg/ml trypsin in DMEM containing 4.5 mg/ml glucose and 80 U/ml DNase at 37°C for 20 min. The cells were gently triturated and mixed with NSC medium (DMEM/F12, B27 supplement), 100 U/ml penicillin, and 100 μg/ml streptomycin. After passing through a 70-μm strainer (BD Biosciences), the cells were pelleted at 200*g* for 4 min. The centrifugation step was repeated once. The supernatant was removed, and the cells were resuspended in NSC medium supplemented with 3 nM EGF. Cells were plated on culture dishes and incubated at 37°C. Neurospheres were ready to be split approximately 7 days after plating. Cells from passage 2 or 3 were routinely used in all in vitro experiments. To split neurosphere cultures, the spheres were collected by centrifugation at 200*g* for 4 min, resuspended in 0.5 ml trypsin/EDTA in 1× HBSS, incubated at 37°C for 2 min, and triturated gently to aid dissociation. Following an additional 3-min incubation at 37°C and trituration, the cells were pelleted at 220*g* for 4 min and resuspended in freshly prepared NSC medium supplemented with 3 nM EGF and 1 nM bFGF. Cells were plated and incubated at 37°C. The rat striatal embryonic cell line ST14A (Cattaneo and Conti, 1998) was grown in DMEM + glutamax-I containing 10% FCS. The cells were split at a ratio of 1:5 twice per week.

ATP Assay

Intracellular ATP levels have been shown to correlate with cell number (Crouch et al., 1993). Neurospheres were split and seeded in NSC medium as a single-cell suspension in 96-well plates (Corning), 10,000 cells/well. Exendin-4 was added, each dose to four parallel wells (quadruplicates), and incubated at 37°C for 4 days. Intracellular ATP was measured with an ATP kit according to the manufacturer's instructions (BioThema, Sweden). The ST14A cells were seeded at 2,000 cells/well in 96-well plates in DMEM/F12 containing N2 supplemented with 1% FCS for 2 hr until the cells had attached. After cell attachment, the medium was changed to serum-free medium, and 100 nM exendin-4 was added. The cells were incubated at 37°C for 3 days and analyzed for ATP content as described above.

In Vitro Bromodeoxyuridine Incorporation Assay

To assay bromodeoxyuridine (BrdU) on adherent cells, neurospheres were split and seeded on poly-D-lysine-coated 96-well plates (Corning), 30,000 cells/well, passage 3, in NSC medium supplemented with 1% FCS. After 4 hr, the medium was changed to serum-free medium, and 100 nM of exendin-4 was added. The cells were incubated at 37°C for 3 days. To assay BrdU incorporation in neurospheres or in ST14A cells, cell culturing and exendin-4 treatment was performed as described for the ATP assay. During the final 24 hr of the experiment, a final concentration of 10 μM BrdU was present. BrdU quantification was analyzed by ELISA according to the manufacturer's instructions in the kit (Roche).

Cell Counts

Adherent NSC cultures were prepared as described above but were incubated with 1% FCS for 24 hr before changing the media. The cells were treated with GLP-1 (7–37) for 3 days, and the cells were rinsed with PBS and fixed with 4% formaldehyde in PBS for 5 min. After fixation, cells were washed and permeabilized with 0.1% Triton X-100 in PBS and stained with 3 nM DAPI. The DAPI-stained cells were analyzed and counted in the InCell Analyzer 1000 system (GE Healthcare). Image analysis was performed in InCell Analyzer Workstation version 3.3. The Dual-Area Object analysis algorithm was used. For each experiment and each staining, a threshold level of DAPI signal in the nuclear area is determined manually and used, together with nuclear size, to define nuclei and applied to count cell nuclei and thus cell number. In each well, four nonoverlapping areas were analyzed.

In Vitro Differentiation Assay

NSC were plated on poly-D-lysine in 24-well plates, 200,000 cells/well, in NSC medium supplemented with 1% FCS. After 24 hr, medium was changed to serum-free medium, and 100 nM exendin-4 was added. Cells were incubated for 6 days, with one medium change and addition of fresh exendin-4 after 3 days. After the incubation period, cells were washed in PBS, fixed with 4% paraformaldehyde (PFA) for 10 min, and washed again. The cells were with 0.1% Tween in PBS and incubated with primary antibodies for 18 hr at 4°C. The following antibodies were used: DCX (1:100), MAP2 (1:500), β-III-tubulin (1:500), and NSE (1:2,000). Cells were rinsed several times with PBS before exposure to appropriate fluorochrome-conjugated secondary antibodies for 2 hr at room temperature. Nuclei were counterstained with Hoechst 33342.

Stained cells were analyzed and counted in the InCell Analyzer 1000. Image analysis was performed in InCell Analyzer Workstation version 3.3 software. The Dual-Area Object analysis algorithm was used. First, nuclei were located based on the image from the Hoechst staining. Second, a 1.6-μm collar was defined around the nucleus, facilitating the detection of perinuclear staining. For each experiment and each staining, a threshold level of signal in the perinuclear area or within the nucleus required to classify the cell as positive was determined manually.

RT-PCR

NSC and lateral ventricle wall (LVW) tissue were collected from of 5–6-week-old mice (C57 black). Total RNA was extracted using the RNeasy mini kit (Qiagen, Valencia, CA), and the RNA was DNase I treated to eliminate possible DNA contamination. The following primer pair was used for GLP-1R detection: 5′-TCAGAGACGGTGCAGAAATG-3′ and 5′-CAGCTGACATTCACGA AGGA-3′. A one-step RT-PCR was performed according to the manufacturer's instruction (Superscript One-Step PCR With Platinum Taq; Invitrogen). Controls for contamination by exogenous or genomic DNA included parallel reactions in which the RT-Taq polymerase mix was replaced by Taq polymerase alone, with or without total RNA. RNA from total mouse brain was used as a positive control. The RT-PCR consisted of one cycle of 50°C for 30 min and 94°C for 2 min; 35 cycles of 94°C for 15 sec, 52°C for 30 sec, 72°C for 15 sec; last cycle 72°C for 7 min. The PCR product was analyzed on a 1.5% agarose gel containing ethidium bromide. The product was sequenced to verify the identity of the band.

GLP-1R Immunohistochemistry

Male Sprague Dawley rats (B&K Universal, Sollentuna, Sweden) weighing about 300 g were housed under standard conditions with feeding and drinking ad libitum. Transcardial perfusion with 4% PFA was performed, brains were frozen in isopentane, and 12-μm coronal sections from the LVW (bregma 1.20; Paxinos and Watson, 1989) were stained immunohistochemically using a rat polyclonal antibody directed toward GLP-1R. Briefly, sections were postfixed in 4% PFA, washed in PBS, treated with 0.3% H_2O_2 in methanol for 20 min, and washed again. Incubation with GLP-1R antibody (1:100) was performed at 4°C overnight in PBS with 0.1% Tween and 10% goat serum. On the following day, sections were washed and incubated for 1 hr at room temperature with biotinylated secondary antibody diluted in 0.1% PBS-Tween. Sections were washed again, and DAB staining was performed according to the Vectastain ABC kit instructions (Vector Laboratories). Tissue sections were counterstained with hematoxylin, dehydrated, placed in xylene overnight, and mounted with xylene-based mounting media.

BrdU or DCX Immunohistochemistry

Male Wistar rats (Harlan-Winkelmann, Germany) weighing about 270 g were housed under standard conditions, with feeding and drinking ad libitum. Animals were injected intraperitoneally (i.p.) twice daily for 7 days with 1 μg/kg exendin-4 and 50 mg/kg BrdU in PBS containing 0.1% RSA for 7 days (N = 10). In further animal experiments, we reduced the dose to 0.1 μg/kg exendin-4, because we observed similar effects on NSC BrdU incorporation at this dose (data not shown).

The vehicle group received BrdU in PBS containing 0.1% RSA (N = 12). Transcardial perfusion with 4% PFA was performed on day 8. After dissection, brains were sectioned at 25 μm coronally through the lateral ventricle (bregma 1.20; Paxinos and Watson, 1989). Immunohistochemistry was performed on free-floating sections, which were denatured in 2 M HCl and incubated with serum to reduce nonspecific binding. Primary antibody, mouse anti-DCX (1:100) and rat monoclonal anti-BrdU (1:100) were incubated with the sections at 4°C overnight. The sections were then stained with biotinylated secondary antibody for 30 min, washed and stained with Vector Elite Kit and fast DAB according to the manufacturer's instructions, and mounted on microscope slides. BrdU-positive cells were counted along the LVW (including the ependymal cell layer and the SVZ). The cell count was divided by a defined distance along the LVW and referred to as numerical density. The mean value for the experimental groups was compared with that of the control group.

6-OHDA Lesions

Male Sprague-Dawley rats weighing 280–350 g were housed in a temperature-controlled room under a 12-hr light/dark cycle, with food and water ad libitum. Thirty minutes prior to surgery, animals were injected intraperitoneally with pargyline (5 mg/kg; monoamine oxidase inhibitor) and desipramine (25 mg/kg; noradrenaline uptake inhibitor). Rats were then placed in a stereotactic frame under general anesthesia (halothane). A small burr hole was made in the right side of the skull. Each animal received a unilateral injection of 4 μg of 6-OHDA (in 2 μl sterile water with 0.1% ascorbic acid) or vehicle into the right medial forebrain bundle at coordinates −2.8 mm from bregma, 2 mm lateral to the midline, and 8.6 mm below the skull according to the atlas of Paxinos and Watson (1989). The 6-OHDA injection was made over a 5-min period using a 5-μl Hamilton syringe. The rats were allowed to recover for 5 weeks following the lesion (Ungerstedt and Arbuthnott, 1970).

Study Design

Two lesion groups consisting of 15 rats each and two sham group of five rats each (i.e., 40 animals in total) were used in the study. One sham group and one lesion group received vehicle, whereas the other sham and lesion group received exendin-4 (0.1 μg/kg exendin-4 in PBS) twice daily for 21 days. The animals were randomly assigned to vehicle vs. exendin-4 groups. During the study, the animals received 0.05 mg/kg s.c. apomorphine and 5 mg/kg i.p. amphetamine once per week for 8 weeks after initiation of drug treatments to measure rotational activity (see Fig. 6).

Rotational Activity

Rotations were measured by counting the total number of rotations during 1 hr. For apomorphine, net contraversive rotations were plotted and for amphetamine, net ipsiversive rotations were plotted. Data derived from automated rotometers were analyzed in GraphPad Prism 3. To select animals with a partial lesion, animals were excluded from the final data analysis based on the following criteria: 1) a rotational response to apomorphine (indicates a full lesion), 2) no rotational response to amphetamine up to week 1 (i.e., <50 net ipsiversive rotations; indicates a nonsufficient lesion), and 3) animals terminated before the end of the study. After application of these exclusion criteria, the final numbers of rats in each group were five in the sham groups and eight in the groups with lesioned animals.

Immunohistochemistry for TH and VMAT2

For each of the 16 animals with a partial 6-OHDA lesion (eight vehicle and eight exendin-4 treated), coronal tissue sections (12 μm) from striatum (bregma +1 to +0.2) and SN (bregma −4.80 to −6.04) were analyzed by immunohistochemistry using antibodies directed toward TH or VMAT2. Briefly, tissue sections were dried, postfixed in 4% paraformaldehyde, washed in PBS, treated with 0.3% H_2O_2 in methanol for 20 min, and washed again. Incubation with TH (1:800) or VMAT2 (1:250) antibody was performed at 4°C overnight in PBS with 0.1% Tween and 10% goat serum. On the following day, sections were washed and incubated for 1 hr at room temperature with biotinylated secondary antibody diluted in 0.1% PBS-Tween. DAB staining was performed according to the Vectastain ABC kit instructions (Vector Laboratories). For each animal, three tissue sections from one level of striatum were stained and analyzed for TH-positive fiber innervation.

To achieve a TH and VMAT2 cell count representative of the whole SN, each animal was analyzed at four and three rostrocaudal levels for the TH and VMAT2, respectively (bregma −4.80 to −6.04). Two tissue sections from each level were quantified by immunohistochemistry. Thus, eight tissue sections were analyzed for each animal for the TH staining, whereas, for the VMAT2 staining, six different sections per animal were counted for positive cells. To compare the effect mediated by exendin-4 vs. vehicle, the number of TH/VMAT2-immunopositive cells on the lesioned (ipsilateral) side of SN was normalized to the nonlesioned side in each tissue section analyzed. The median value of all analyzed sections was calculated for each animal. To evaluate whether the median values of the exendin-4-treated animals were significantly different from the median values of the vehicle-treated animals, the nonparametric Mann-Whitney U-test was performed.

Animal Use and Care

The study was performed according to guidelines of the Karolinska Institutet and was approved by the Animal Ethical Committee (Stockholms norra djurförsöksetiska nämnd, Södra Roslags Tingsrätt, Stockholm, Sweden).

Statistical Analysis

In every in vitro experiment, the effect of the each compound and dose was determined in quadruplicate (four parallel wells) in three different cell preparations. Unpaired Student's *t*-test was carried out in Microsoft Excel 2003 SP2. One-way ANOVA, Fisher's exact test, Dunnett's post hoc test, and Mann-Whitney U-test were carried out in GraphPad Prism for Windows versions 3 and 4.03.

RESULTS

The Adult Rodent Brain SVZ Expresses the GLP-1R

Expression of GLP-1R in the brain during development and adulthood has previously been reported (Campos et al., 1994; Calvo et al., 1995; Goke et al., 1995; Merchenthaler et al., 1999). The presence of GLP-1R in neurogenic regions of the adult brain and in NSC could suggest a role for GLP-1R in adult neurogenesis. We carried out RT-PCR experiments on SVZ tissue dissected from adult mouse brain and on NSC cultures isolated from the LVW expanded as neurospheres (see Materials and Methods). Bands of the expected size were amplified from RNA isolated from whole brain, SVZ tissue, and NSC cultures (Fig. 1A). Sequencing was used to confirm the identity of the bands (corresponding to NCBI No. gi2597977/embAJ001692.1). The negative controls suggested no contamination of DNA of genomic or plasmid origin (data not shown). Real-time

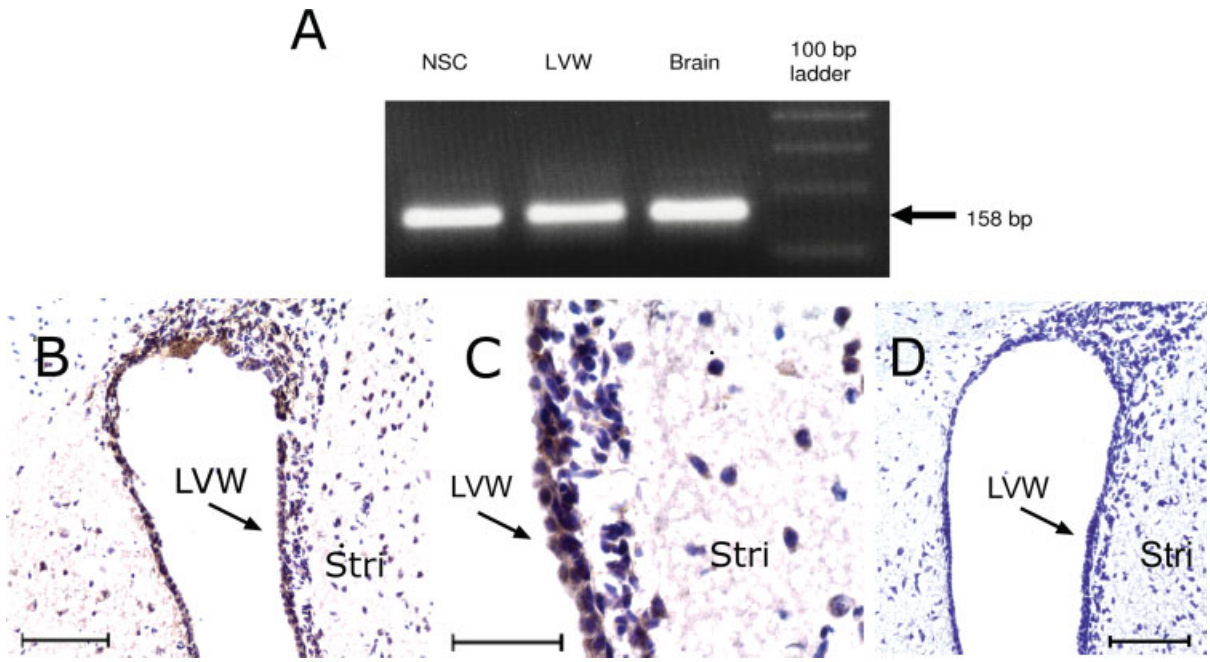

Fig. 1. The GLP-1 receptor is expressed in cultured neural stem cells and in the lateral ventricular wall of adult rodent brains. With primer pairs specific for the glp-1r gene, RT-PCR on total RNA from cultured mouse NSCs, LVW tissue and whole brain gave a single band of the expected size (158 bp; arrow; **A**). Coronal sections of rat brain tissue were stained with an antibody directed toward GLP-1R (brown). GLP-1R expression is seen in the lateral ventricular wall (**B**). In **C**, an enlargement of B is shown. A negative control in absence of GLP-1R antibody with only the secondary antibody is shown in **D**. All sections were counterstained with hematoxylin (blue). NSC, neural stem cell; LVW, lateral ventricle wall; Str, striatum. Scale bars = 80 μm in B; 20 μm in C; 100 μm in D.

PCR was used to confirm these results and verify that glp-1r mRNA was also expressed by NSC cultures grown adherently and expanded as spheres and in tissue from the LVW (data not shown). We analyzed GLP-1R protein expression in the LVW of adult rats by immunohistochemistry. GLP-1R-positive cells were abundant along the SVZ (Fig. 1B,C). These results, together with the positive PCR findings, demonstrate that the GLP-1R mRNA and protein are expressed in neurogenic regions of the adult rodent brain.

Exendin-4 Stimulates In Vitro Neurogenesis

To address whether exendin-4 can modulate adult neurogenesis, we first investigated the effect of this peptide on NSC in vitro. NSC, expanded as neurospheres, were dissociated and treated with exendin-4 for 4 days. To analyze whether exendin-4 affects cell number in vitro, we used an assay measuring intracellular ATP levels, previously shown to correlate to cell number (Crouch et al., 1993). Figure 2A shows a statistically significant, dose-dependent increase in the amount of ATP, and hence cell number, in response to exendin-4 treatment compared with the vehicle control. We also employed a BrdU incorporation assay that allows detection of DNA synthesis to quantify the number of proliferating cells in our cultures (Taupin, 2007). Neurospheres were treated with exendin-4 for 3 days and BrdU was added for the final 24 hr. Figure 2C shows that exendin-4 treatment led to a statistically significant increase in cellular BrdU incorporation compared with the vehicle control, an increase that was also evident in NSC grown adherently (Fig. 2E). Some variations in the extent of cell number increase and BrdU incorporation in response to exendin-4 treatment were observed between different primary isolations, with significant effects being obtained in approximately 80% of all experiments performed. In addition to the effects on NSC isolated from the adult SVZ, exendin-4 was also capable of significantly increasing intracellular ATP levels and BrdU incorporation in cultures of the rat embryonic striatal-derived stem cell line ST14A (Cattaneo and Conti, 1998; Fig. 2B,D). Exendin-4 is a selective agonist for the GLP-1R (Goke et al., 1993; Thorens et al., 1993; Wheeler et al., 1993); however, to add credence to the notion that the effects of exendin-4 are exerted through the GLP-1R, the receptor's endogenous ligand GLP-1 (7–37) was also tested. Treatment of NSC with GLP-1 (7–37) at 100 nM and 1,000 nM was found to increase the total cell number significantly compared with control (Fig. 2F). Thus, exendin-4 causes an increase of cell number in adult mouse NSC cultures, grown as neurospheres or adherently, as measured by ATP levels or by BrdU incorporation, as well as in the rat embryonic striatal-derived stem cell line ST14A. To investigate whether exendin-4 is capable of stimulating

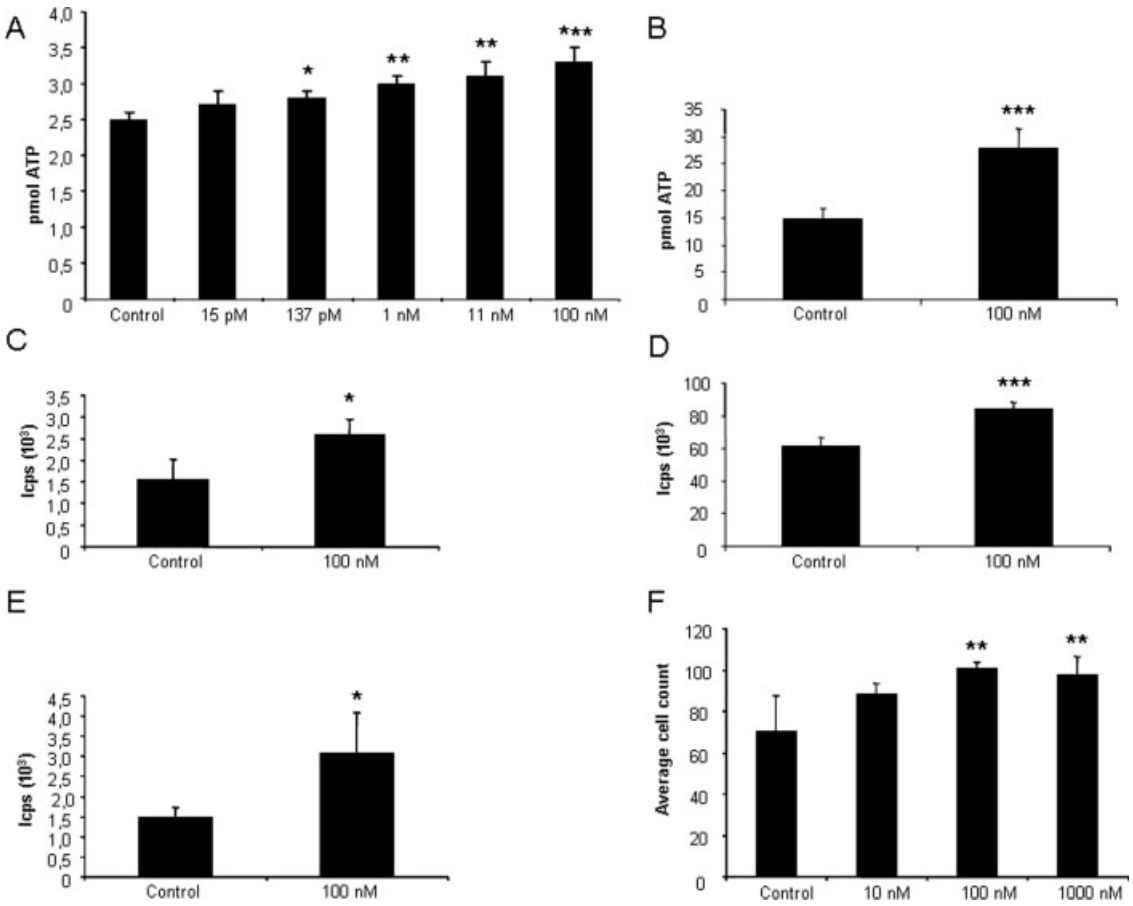

Fig. 2. Exendin-4 treatment increases cell number in vitro. NSCs grown as neurospheres were treated with increasing concentrations of exendin-4 for 4 days in vitro followed by quantification of intracellular ATP, a measure of cell number. A dose-dependent, statistically significant increase in ATP is seen with increasing exendin-4 doses (**A**). NSCs, grown in suspension (**C**) or adherently (**E**), were exposed to 100 nM exendin-4 for 3 days. BrdU was present during the last 24 hr. Statistically significant increase in BrdU incorporation, as measured by ELISA (lcps = light count per second), is demonstrated. Statistically significant increases in ATP levels (**B**) and BrdU incorporation (**D**) were also observed in the rat stem cell line ST14A when treated with 100 nM exendin-4 for 3 days. After a 3-day treatment of adherent NSC cultures with the endogenous GLP-1R ligand GLP-1 (7–37), an increase in cell number, as quantified using the InCell Analyzer, could be demonstrated (**F**). Columns represent mean values, whereas error bars represent SD of the quadruplicate measurements in the single representative experiment. $\star P < 0{,}05$, $\star\star P < 0{,}01$, $\star\star\star P < 0{,}001$, one-way ANOVA (A,F) or unpaired Student's *t*-test (B–E).

differentiation of in-vitro-cultured NSC toward a neuronal phenotype, we analyzed expression phenotype by immunocytochemistry. The number of labelled and unlabelled cells was quantified by using an automated image acquisition and analysis system (see Materials and Methods). NSC plated adherently and exposed overnight to serum were treated with exendin-4 for 6 days and were analyzed for β-III-tubulin, MAP2, DCX, and NSE expression by immunocytochemistry. Figure 3 and Table I show that the proportion of cells in the population expressing the neuronal marker β-III-tubulin increased from 3% to 15%. Similarly, in the population counted, MAP2-positive cells increased from 1% to 3% and NSE-positive cells from 7% to 24% upon exendin-4 treatment (Fig. 3, Table I). The number of cells expressing the early neuronal marker DCX was not increased at this time point (Table I). In summary, these results indicate that exendin-4 is active on in-vitro-cultured NSC by triggering both proliferation and neuronal differentiation.

Exendin-4 Stimulates Neurogenesis in the SVZ of the Adult Rat Brain

Our results showing that exendin-4 is a regulator of NSC fate and number in vitro suggest that exendin-4 could act as a modulator of neurogenesis in vivo. To address this question, we first investigated whether exendin-4 was able to promote in vivo cell proliferation in the SVZ of adult rats. Adult rats were injected i.p. with exendin-4 twice daily for 7 days. BrdU was coadministered to detect DNA synthesis. Brains were sectioned coronally through the lateral ventricle, sections were im-

munostained for BrdU, and the stained cells were counted. There is an increase in BrdU-positive cells along the LVW after exendin-4 treatment compared with vehicle (Fig. 4A). Quantification shows that exendin-4 almost doubled the number of BrdU-positive cells in the SVZ compared with the vehicle control (Fig. 4B). To assess whether exendin-4 treatment increases the formation of new neurons in vivo, striatal coronal sections were immunostained with DCX, a marker for neuroblasts. In the adult brain, DCX is expressed mainly in the SVZ, rostral migratory stream, and hippocampus, but some DCX-expressing cells also migrate from the SVZ toward the medial striatum. The detection of DCX in the striatum has been shown to reflect levels of adult neurogenesis (Arvidsson et al., 2002; Couillard-Despres et al., 2005). We found many DCX-positive cells in the SVZ, but reliable quantification was difficult because of the high density of DCX expression. However, DCX-positive cells were also observed, and could be quantified, in the medial striatum adjacent to the SVZ. We found that exendin-4 treatment increased the number of DCX-positive cells by about 1.7-fold compared with vehicle control ($P < 0.01$; Fig. 5A). A representative picture of DCX-positive cells from medial striatum adjacent to the SVZ is shown in Figure 5B,C. Altogether, our results show that exendin-4 can stimulate neurogenesis from adult NSC in vivo.

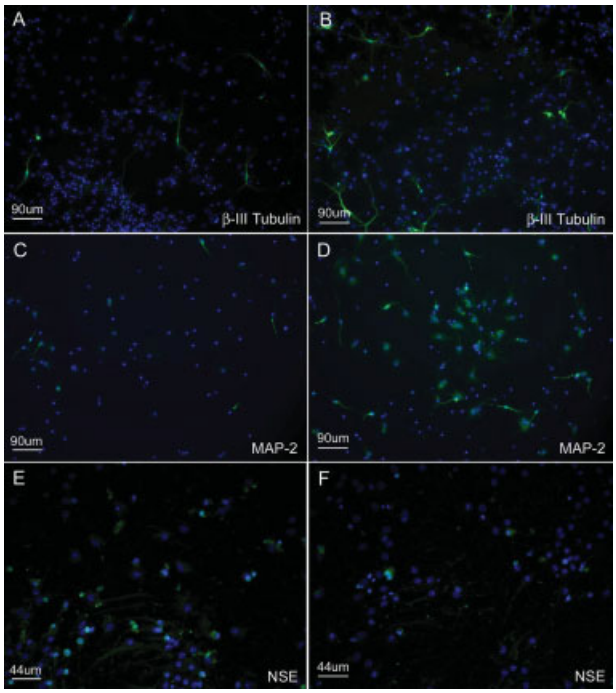

Fig. 3. Exendin-4 increases neuronal differentiation in cultured adult mouse neurospheres (NSC). NSCs were treated with 100 nM exendin-4 for 6 days (**B,D,F**) and compared with control cells (**A,C,E**). Cells were fixed and stained with antibodies for β-III-tubulin (A,B), MAP2 (C,D), and neural specific enolase (E,F).

Exendin-4 Treatment Reduces Amphetamine-Induced Rotations in the 6-OHDA Model of Parkinson's Disease

To investigate the potential of exendin-4 to elicit recovery of function in a model of PD, we chose a PD model in which the animals have a partial, unilateral loss of dopaminergic neurons. The lesion is induced by a single injection of 6-OHDA in the median forebrain bundle (see Materials and Methods). Upon amphetamine stimulation, these animals will display ipsiversive rotational behavior as a result of the imbalance in DA release resulting from the unilateral loss of DA cells. This allows the functional effects of a compound tested in this model to be quantified by counting the number of amphetamine-induced rotations (Ungerstedt and Arbuthnott, 1970). Two sham groups, vehicle or exendin-4 treated, were included as controls. The experimental setup is outlined in Figure 6.

Prior to the initiation of exendin-4 or vehicle treatment, the number of amphetamine-induced net ipsiversive rotations was 275 ± 51 in the group of lesioned animals that were to receive vehicle only. In the group of lesioned animals to receive exendin-4, the number of rotations was 254 ± 63. The difference between the groups was not significant ($P > 0.05$, unpaired *t*-test; Fig. 7). In the group of lesioned animals receiving vehicle only, weekly amphetamine challenges had no effect on rotation compared with the response before the initiation of treatment (all $P > 0.05$, one-way repeated-measures ANOVA followed by Dunnett's test; Fig. 7). In lesioned animals that received exendin-4, however, weekly amphetamine challenges caused a significant reduction in net ipsiversive rotations at weeks 3–8 compared with the response before the initiation of treat-

TABLE I. Exendin-4 Induces Neuronal Differentiation in Cultured Adult Mouse Neural Stem/Progenitor Cells*

	β-III-Tubulin		MAP2		NSE		Doublecortin	
	Ctrl	Ex	Ctrl	Ex	Ctrl	Ex	Ctrl	Ex
Counted cells	2,905	3,397	1,309	1,117	1,006	1,129	2,456	2,856
Positive cells	89	521	15	35	66	271	129	135
Percentage positive cells	3	15	1	3	7	24	5	5
Fisher's exact test	$P < 0.0001$		$P < 0.001$		$P < 0.0001$		$P > 0.05$	

*Quantification of stained NSC in Figure 3 using the InCell Analyzer 1000. Twelve randomized fields/well were counted. Fisher's exact test was used for data analysis. Ctrl, control; ex, exendin-4.

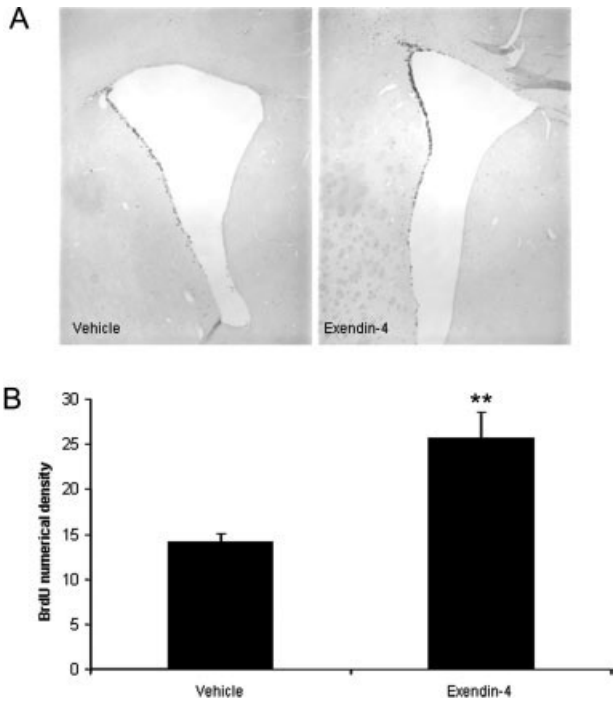

Fig. 4. Exendin-4 treatment increases the number of BrdU-positive cells in the subventricular zone. After 7 days of i.p. injections of exendin-4 and BrdU, rat brains were analyzed for signs of NSC proliferation in vivo. A representative micrograph shows increased BrdU labelling of the subventricular zone in the exendin-4 treated animals compared with the control (**A**). To quantify the effect, cells in the SVZ along a distance of 600 μm were counted in two sections, starting in the dorsolateral corner of the lateral ventricle (**B**). Numerical density is defined as number of cells counted, divided by the distance. Error bars represents SEM values. $^{**}P < 0{,}01$, Student's *t*-test.

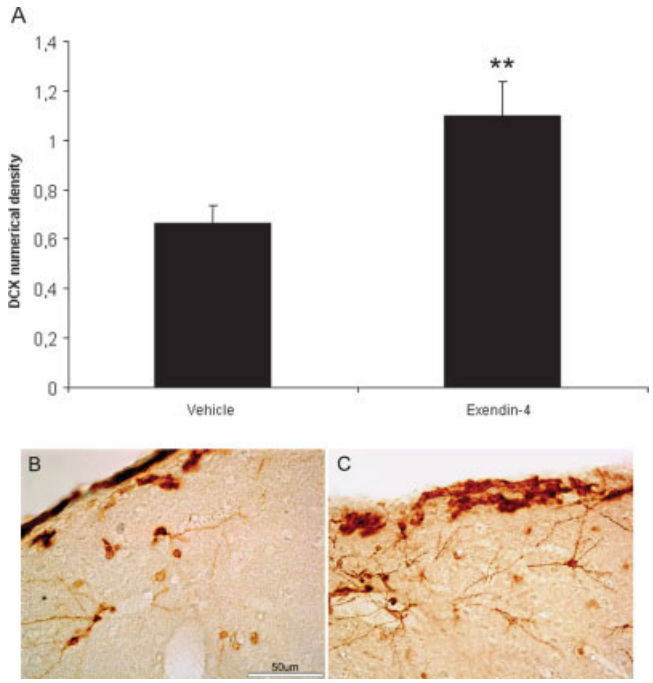

Fig. 5. Exendin-4 treatment increases the number of neuronal precursors in the medial striatum. After 7 days of i.p. injections of exendin-4, rat brains were analyzed for DCX-positive cells in the medial striatum. The number of immunoreactive cells, counted in the striatum adjacent to the SVZ from two sections per animal, was significantly higher in exendin-4-treated animals compared with untreated controls (**A**). A representative picture of DCX-stained cells is shown in **B,C**. Numerical density = number of cells counted divided by the area. Error bars represents SEM values. $^{**}P < 0{,}01$, Student's *t*-test.

ment (all $P < 0.01$, one-way repeated-measures ANOVA followed by Dunnett's test; Fig. 7). The reduction at week 8 was 78% compared with pretreatment levels. Comparison of the vehicle-treated lesioned group with the exendin-4-treated lesioned group showed a significant difference in ipsiversive rotations at weeks 3–8 (all $P < 0.05$, unpaired *t*-test; Fig. 7). Amphetamine (5 mg/kg i.p.) did not induce rotation in either of the sham-operated groups at any stage during the study. In summary, exendin-4 treatment resulted in an almost complete normalization of amphetamine-induced rotations in the 6-OHDA model of PD.

Exendin-4 Increases the Number of TH/VMAT2-Positive Neurons in the 6-OHDA Animal Model

To investigate the mechanisms responsible for the exendin-4-induced recovery in the 6-OHDA animal model, we performed immunohistochemical characterization of the SN. First, we determined the number of cells positive for TH, the rate-limiting enzyme for the DA synthesis, in tissue collected 5 weeks after the last exendin-4 treatment (see Fig. 6 for study design). Sixteen animals (eight vehicle and eight treated with exendin-4) were analyzed immunohistochemically with an antibody directed toward TH. Neurons positive for TH were counted in eight coronal tissue sections taken at different levels of the SN (see Materials and Methods for further details). To quantify the staining, we counted the number of TH neurons on the ipsilateral side of the SN and normalized to the cell counts on the contralateral side. Interestingly, the number of TH-positive neurons on the ipsilateral side was significantly higher ($P < 0.05$) in the group treated with exendin-4 (Table II). The normalized median cell counts for the exendin-4-treated animals were 0.24 (min 0.12, max 0.60) and for the vehicle-treated animals 0.12 (min 0.079, max 0.44). Thus, exendin-4 treatment resulted in a doubling of TH-positive neurons in the ipsilateral SN. The number of TH-positive neurons on the nonlesioned contralateral side was not affected by the exendin-4 treatment. Figure 8 shows representative examples of TH staining from the contralateral and ipsilateral SN in vehicle- and exendin-4-treated animals, respectively. The increased numbers of TH-positive cells in treated animals correlated with increased TH-positive fiber staining in striatum (data not shown).

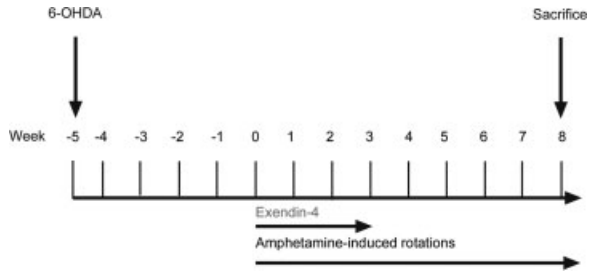

Fig. 6. Study design. Four groups of rats were partially lesioned with unilateral injections of 6-OHDA in the medial forebrain bundle. The lesion was allowed to stabilize for 5 weeks. Each group received vehicle or drug treatment twice per day for 21 days. During the study, the animals received 5 mg/kg amphetamine intraperitoneally once per week for 8 weeks after initiation of drug treatments, and rotational activity was measured weekly.

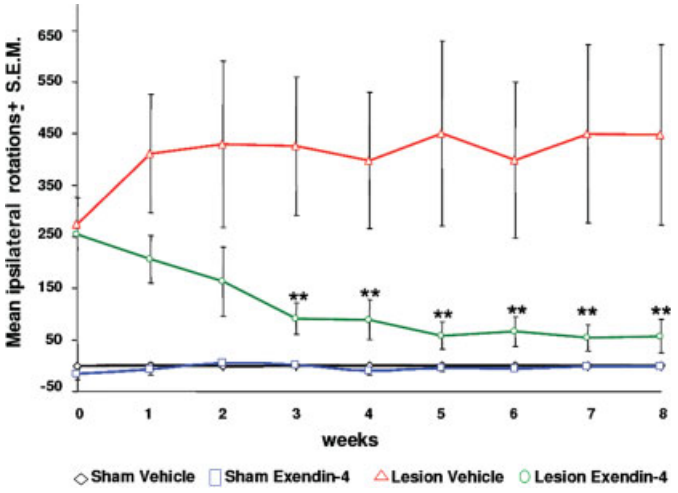

Fig. 7. Functional recovery in the 6-OHDA model of PD following exendin-4 treatment. Partially 6-OHDA lesioned rats were allowed to recover for 5 weeks before exendin-4 treatment (3 weeks; twice daily, intraperitoneally). Amphetamine-induced rotations were monitored weekly, starting at the beginning of the treatment, for 8 weeks, and a significant effect of exendin-4 was observed from week 3. $\star\star P < 0.01$ vs. week 0; one-way repeated-measures ANOVA followed by Dunnett's test. $\star P < 0.05$ vs. lesion + vehicle; unpaired *t*-test.

To characterize further the effect of exendin-4 on DA neurons, we examined the expression of VMAT2. VMAT2 is a key regulator of neurotransmission and is responsible for the proper storage and handling of DA, including filling of synaptic vesicles with the neurotransmitter. It is thought that VMAT2 serves a neuroprotective role in the DA system by sequestering DA into vesicles, which prevents autooxidation of cytosolic DA and resulting free radical generation (Miller et al., 1999). The treatment with exendin-4 resulted in a significant increase in the number of VMAT2-stained cells, confirming the results of the TH immunostaining (Fig. 9).

TABLE II. TH and VMAT2 Cell Counts in Substantia Nigra[†]

Treatment	TH ipsi/contra	VMAT2 ipsi/contra	*N*
Median vehicle	0.12 (0.10–0.13)	0.074 (0.03–0.12)	8
Median exendin-4	0.24★ (0.16–0.51)	0.21★ (0.12–0.24)	8

[†]Values are cell counts on the ipsilateral (lesioned) side divided by cell counts on the contralateral (nonlesioned) side. Median values for each group; the 25^{th}–75^{th} percentile are shown in parentheses. Each animal's data were collected from eight (TH) or six (VMAT2) serial sections from substantia nigra between bregma –4.80 and –6.04.
★Cell counts for both TH and VMAT2 are statistically higher (Mann-Whitney unpaired test; $P < 0.05$) in the exendin-4-treated compared with the vehicle-treated animals.

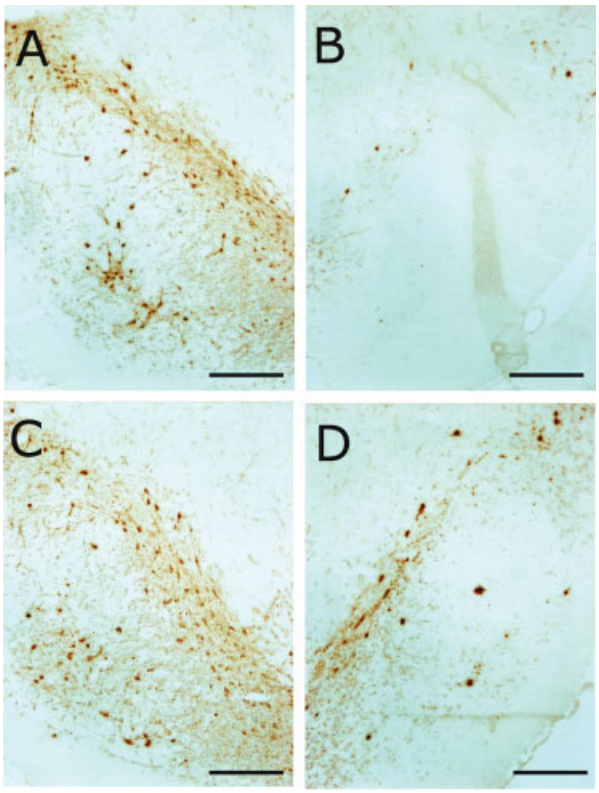

Fig. 8. Increased number of TH-positive neurons in the animals treated with exendin-4. TH immunostaining of coronal sections taken from the substantia nigra at week 8. Representative examples of stainings in the ipsilateral (**B,D**) and contralateral (**A,C**) SN in animals treated with vehicle (A,B) or exendin-4 (C,D). Scale bars = 100 μm.

In more detail, the treatment with exendin-4 significantly ($P < 0.05$) increased the VMAT2-positive neurons; the normalized cell counts for exendin-4 were 0.21 (min 0.08, max 0.37) compared with 0.074 (min 0.017, max 0.37) for the vehicle-treated animals (Table II). In summary, our results show that exendin-4 treatment results in an increased number of TH- and VMAT2-positive neurons in the 6-OHDA animal model of PD.

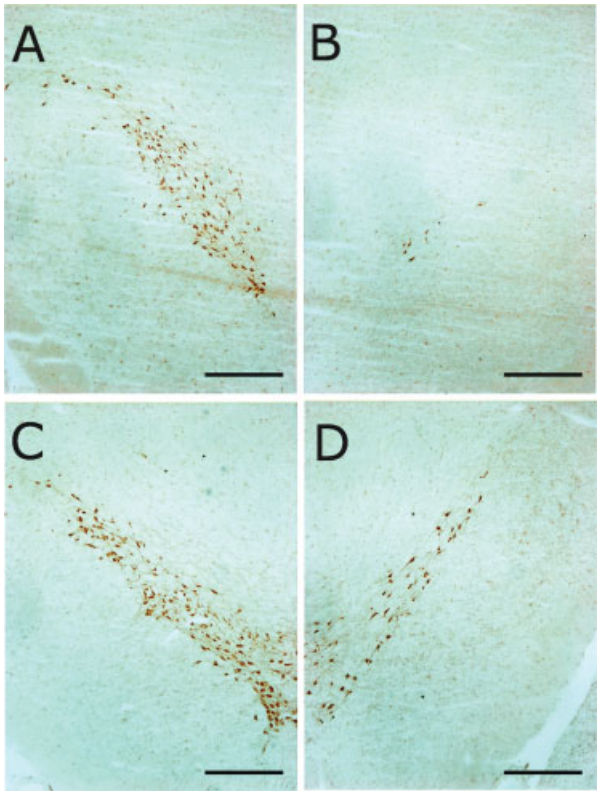

Fig. 9. Increased number of VMAT2-positive neurons in the animals treated with exendin-4. VMAT2 immunostaining of coronal sections from substantia nigra. Representative examples of stainings in the ipsilateral (**B,D**) and contralateral (**A,C**) substantia nigra in animals treated with vehicle (A,B) or exendin-4 (C,D) are shown. The tissue sections shown in this figure are consecutive sections taken from the same animal as shown in Figure 8. Scale bars = 100 μm.

DISCUSSION

Previously published work has shown that exendin-4 can promote β-cell proliferation and islet neogenesis (Li et al., 2003; Gedulin et al., 2005). It has also been demonstrated that exendin-4 is able to enhance the differentiation of insulin-producing cells from embryonic stem cells (Bonner-Weir and Weir, 2005); however, no evidence for regenerative activity in the CNS or NSC stimulation has been previously reported. In this study, we investigated the potential of exendin-4 to modulate the activity of adult NSC. First, we showed that the receptor for exendin-4, GLP-1R, is expressed in the mouse SVZ, a site for NSC in the adult brain. With different methods, we have shown exendin-4 to influence NSC culture growth significantly. An increase in overall cell number and in the number of cells undergoing mitosis was found in NSC cultures grown as neurospheres or as adherent monolayers and also in a rat embryonic striatal-derived stem cell line, ST14A. The endogenous GLP-1R ligand GLP-1 (7–37) (Kieffer and Habener, 1999) was also effective in promoting an increase in cell number. In an attempt to confirm that the GLP-1R is responsible for the effects, we also tested two compounds described in the literature as GLP-1R antagonists, exendin-4 (3–39) and exendin-4 (9–39) (Montrose-Rafizadeh et al., 1997a). Intriguingly, when tested in our experimental systems, the 3–39 and the 9–39 forms of exendin-4 significantly increased the cell numbers (data not shown). Interestingly, previous studies have shown that exendin-4 (9–39) can act as a GLP-1R agonist rather than as an antagonist in several cell types (Montrose-Rafizadeh et al., 1997b; Yang et al., 1998; Gonzalez et al., 2005), something that requires consideration when drawing conclusions. Taken together, our data show that exendin-4 can stimulate adult NSC as well as embryonic striatal stem cells and that the effects are likely to be GLP-1R mediated.

To investigate the differentiation potential of NSC upon exendin-4 stimulation, the expression of certain markers for neuronal differentiation was studied. Exendin-4 treatment caused an increase in the percentage of cells expressing the neuronal markers MAP2, β-III-tubulin, and NSE. This indicates that, at least in vitro, differentiation along the neuronal lineage is possible.

To study whether the effects of exendin-4 found in vitro on NSC also occur in neurogenic regions of the adult brain, adult mice (data not shown) or rats were treated with exendin-4. We found that exendin-4 promoted a significant increase in the number of cells that incorporate BrdU in the SVZ as well as in the number of cells expressing the early neuronal marker DCX in the medial striatum adjacent to the SVZ. However, it should be noted that our experiments do not rule out that survival of NSC could contribute to the neurogenic net effects by exendin-4 in vitro or in vivo. Work by Arvidsson et al. (2002) shows that newly formed cells in the SVZ have the potential to become DCX-expressing neuroblasts with the ability to migrate into the medial striatum. Interestingly, the in vitro differentiation experiments show that exendin-4 increases the proportion of cells expressing the neuronal markers β-III-tubulin, MAP2, and NSE but not DCX. In contrast, after exendin-4 treatment there was a significant increase in the DCX-immunopositive cells in vivo. One explanation for this discrepancy is that the time point analyzed in vitro was not optimal for studying DCX gene expression, which is known to be transient during neuronal differentiation in vivo. Another possibility is that proper neuronal differentiation does not occur in the in vitro system, perhaps because of the lack of proper extrinsic or intrinsic signals.

Neurogenesis has been shown to occur throughout life in discrete regions of the CNS in mammals (for review see Carlen et al., 2006). This slow physiological turnover of neurons in the adult brain suggests a functional role for NSC in the CNS. Endogenous neurogenesis can be regulated by, for example, physical exercise, enriched environment, injury (stroke), and growth factors (for review see Emsley et al., 2005; Taupin, 2006). For instance, after ischemic brain injury, it has been

shown that i.c.v.-administered growth factors EGF, FGF-2, G-CSF, and GDNF increase neurogenesis from the adult SVZ. The new cells were able to integrate functionally (Nakatomi et al., 2002; Schneider et al., 2005; Kobayashi et al., 2006). Thus, the identification of compounds that can selectively trigger NSC to proliferate and to differentiate into desired phenotypes could be useful for the treatment of neurological diseases. Such compounds could be used for expanding subsets of defined cells populations for transplantation therapies or be used to stimulate adult neurogenesis.

Exendin-4 is used for the treatment of diabetes type II. Also, exendin-4 passes the blood–brain barrier, at least in mice (Kastin and Akerstrom, 2003), and could possibly have therapeutic CNS effects also after peripheral administration. Although additional experimental evidence is needed, this suggests a potential role for exendin-4 in the treatment of, e.g., Parkinson's disease, stroke, or Alzheimer's disease based on stimulation of neurogenesis.

It is interesting to note that exendin-4 has been shown to act as a neurotrophic factor, improving memory/cognition (During et al., 2003; Perry et al., 2003). Our study, showing that exendin-4 stimulates neurogenesis in the SVZ, suggests that the neurogenic effects by exendin-4 may contribute to the restorative effect reported. In addition, preliminary data show that exendin-4 induces neurogenesis also in the hippocampus (data not shown).

Neurogenesis in the SN is controversial but is supported by independent publications (Zhao et al., 2003; Shan et al., 2006). Our finding that exendin-4 stimulates adult neurogenesis, together with the finding that this peptide can directly induce TH transcription in catecholamine neurons (Yamamoto et al., 2003), motivated a study to see whether exendin-4 is capable of inducing functional recovery in animal models of PD and thus be considered for the treatment of PD. PD is a pathology of the CNS that is believed to develop through a gradual decline in the number of DA neurons in the SN possibly caused by an abnormally rapid rate of cell death (Marsden, 1990). Our observation of an exendin-4-mediated functional recovery in the 6-OHDA model points to interesting possibilities. As shown in Figure 7, effects of exendin-4 can be observed relatively soon after initiation of treatment. The improvement continues throughout the exendin-4 treatment period and, remarkably, persists for another 5 weeks in the absence of the treatment. Thus, this seems likely to be a plastic rather than a transitory effect and suggests that exendin-4 is indeed triggering a stable change in the brain by improving the course of the pathology rather than just exerting a symptomatic and acute effect. The increase in the number of neurons positive for two DA markers, TH and VMAT2, reinforces our hypothesis that exendin-4 is acting as a disease-modifying molecule. Interestingly, Van Kampen and Eckman (2006) have shown that SN neurogenesis can be pharmacologically stimulated following treatment with the dopamine D3 receptor agonist 7-OH-DPAT. The presence of a slow physiological turnover of neurons in the adult SN is very intriguing and points to a functional role for neural stem cells in the brain that might be pharmacologically regulated, thus offering an attractive way to treat this severe pathology of the CNS (Borta and Hoglinger, 2007). However, whether neurogenesis can take place directly in the adult SN or whether newborn cells in the SN originate from the LVW is still an area of scientific debate (Mohapel et al., 2005). There may be additional explanations for the increase of TH/VMAT2-positive cells caused by exendin-4. For instance, this effect could also be a result from a phenotypic shift of preexisting TH-negative neurons in the SN, as was recently proposed for striatal neurons of MPTP-treated primates (Tande et al., 2006). An additional component of the effect mediated by exendin-4 could be a trophic effect on remaining dopaminergic neurons. Although the lesion we obtained with 6-OHDA was aimed to be a stable lesion of 70% of DA neurons, we cannot rule out that some of the lesioned DA neurons in the SN can reappear. In this case, the surviving DA neurons might represent a direct target for exendin-4. Continued studies are needed to elucidate the still debated role of adult neurogenesis (Meshi et al., 2006; Nygren et al., 2006; Saxe et al., 2006; Scharfman and Hen, 2007) and the potential of neurogenic compounds for the treatment of brain diseases and injuries.

In conclusion, our study shows that exendin-4 is able to induce proliferation and differentiation in vitro and in vivo of NSC from the adult SVZ and indicates a role for exendin-4 as modulator of adult neurogenesis. We also show that exendin-4 is able to induce a substantial, prolonged, and stable recovery of locomotor function in the 6-OHDA rat model of PD as well as an increase in the number of TH/VMAT2-positive cells in the SN. Once fully clarified, the molecular mechanisms underlying the effects reported here may open new avenues toward novel therapeutics for PD.

ACKNOWLEDGMENTS

We thank Drs. Georg Kuhn and Jonas Frisén for discussions and comments and Drs. Alan Crossman and Michael Hill at MOTAC Neuroscience for valuable contributions.

REFERENCES

Arvidsson A, Collin T, Kirik D, Kokaia Z, Lindvall O. 2002. Neuronal replacement from endogenous precursors in the adult brain after stroke. Nat Med 8:963–970.

Bonner-Weir S, Weir GC. 2005. New sources of pancreatic beta-cells. Nat Biotechnol 23:857–861.

Borta A, Hoglinger GU. 2007. Dopamine and adult neurogenesis. J Neurochem 100:587–595.

Calvo JC, Yusta B, Mora F, Blazquez E. 1995. Structural characterization by affinity cross-linking of glucagon-like peptide-1(7–36)amide receptor in rat brain. J Neurochem 64:299–306.

Campos RV, Lee YC, Drucker DJ. 1994. Divergent tissue-specific and developmental expression of receptors for glucagon and glucagon-like peptide-1 in the mouse. Endocrinology 134:2156–2164.

Carlen M, Meletis K, Barnabe-Heider F, Frisen J. 2006. Genetic visualization of neurogenesis. Exp Cell Res 312:2851–2859.

Cattaneo E, Conti L. 1998. Generation and characterization of embryonic striatal conditionally immortalized ST14A cells. J Neurosci Res 53:223–234.

Couillard-Despres S, Winner B, Schaubeck S, Aigner R, Vroemen M, Weidner N, Bogdahn U, Winkler J, Kuhn HG, Aigner L. 2005. Doublecortin expression levels in adult brain reflect neurogenesis. Eur J Neurosci 21:1–14.

Crouch SP, Kozlowski R, Slater KJ, Fletcher J. 1993. The use of ATP bioluminescence as a measure of cell proliferation and cytotoxicity. J Immunol Methods 160:81–88.

During MJ, Cao L, Zuzga DS, Francis JS, Fitzsimons HL, Jiao X, Bland RJ, Klugmann M, Banks WA, Drucker DJ, Haile CN. 2003. Glucagon-like peptide-1 receptor is involved in learning and neuroprotection. Nat Med 9:1173–1179.

Egan JM, Clocquet AR, Elahi D. 2002. The insulinotropic effect of acute exendin-4 administered to humans: comparison of nondiabetic state to type 2 diabetes. J Clin Endocrinol Metab 87:1282–1290.

Emsley JG, Mitchell BD, Kempermann G, Macklis JD. 2005. Adult neurogenesis and repair of the adult CNS with neural progenitors, precursors, and stem cells. Prog Neurobiol 75:321–341.

Eng J, Kleinman WA, Singh L, Singh G, Raufman JP. 1992. Isolation and characterization of exendin-4, an exendin-3 analogue, from Heloderma suspectum venom. Further evidence for an exendin receptor on dispersed acini from guinea pig pancreas. J Biol Chem 267:7402–7405.

Gage FH, Ray J, Fisher LJ. 1995. Isolation, characterization, and use of stem cells from the CNS. Annu Rev Neurosci 18:159–192.

Gedulin BR, Nikoulina SE, Smith PA, Gedulin G, Nielsen LL, Baron AD, Parkes DG, Young AA. 2005. Exenatide (exendin-4) improves insulin sensitivity and β-cell mass in insulin-resistant obese fa/fa Zucker rats independent of glycemia and body weight. Endocrinology 146:2069–2076.

Goke R, Fehmann HC, Linn T, Schmidt H, Krause M, Eng J, Goke B. 1993. Exendin-4 is a high potency agonist and truncated exendin-(9–39)-amide an antagonist at the glucagon-like peptide 1-(7–36)-amide receptor of insulin-secreting beta-cells. J Biol Chem 268:19650–19655.

Goke R, Larsen PJ, Mikkelsen JD, Sheikh SP. 1995. Distribution of GLP-1 binding sites in the rat brain: evidence that exendin-4 is a ligand of brain GLP-1 binding sites. Eur J Neurosci 7:2294–2300.

Gonzalez N, Acitores A, Sancho V, Valverde I, Villanueva-Penacarrillo ML. 2005. Effect of GLP-1 on glucose transport and its cell signalling in human myocytes. Regul Pept 126:203–211.

Greig NH, Holloway HW, De Ore KA, Jani D, Wang Y, Zhou J, Garant MJ, Egan JM. 1999. Once daily injection of exendin-4 to diabetic mice achieves long-term beneficial effects on blood glucose concentrations. Diabetologia 42:45–50.

Kastin AJ, Akerstrom V. 2003. Entry of exendin-4 into brain is rapid but may be limited at high doses. Int J Obes Rel Metab Disord 27:313–318.

Kieffer TJ, Habener JF. 1999. The glucagon-like peptides. Endocr Rev 20:876–913.

Kieffer TJ, McIntosh CH, Pederson RA. 1995. Degradation of glucose-dependent insulinotropic polypeptide and truncated glucagon-like peptide 1 in vitro and in vivo by dipeptidyl peptidase IV. Endocrinology 136:3585–3596.

Knauf C, Cani PD, Perrin C, Iglesias MA, Maury JF, Bernard E, Benhamed F, Gremeaux T, Drucker DJ, Kahn CR, Girard J, Tanti JF, Delzenne NM, Postic C, Burcelin R. 2005. Brain glucagon-like peptide-1 increases insulin secretion and muscle insulin resistance to favor hepatic glycogen storage. J Clin Invest 115:3554–3563.

Kobayashi T, Ahlenius H, Thored P, Kobayashi R, Kokaia Z, Lindvall O. 2006. Intracerebral infusion of glial cell line-derived neurotrophic factor promotes striatal neurogenesis after stroke in adult rats. Stroke 37:2361–2367.

Kolterman OG, Buse JB, Fineman MS, Gaines E, Heintz S, Bicsak TA, Taylor K, Kim D, Aisporna M, Wang Y, Baron AD. 2003. Synthetic exendin-4 (exenatide) significantly reduces postprandial and fasting plasma glucose in subjects with type 2 diabetes. J Clin Endocrinol Metab 88:3082–3089.

Li Y, Hansotia T, Yusta B, Ris F, Halban PA, Drucker DJ. 2003. Glucagon-like peptide-1 receptor signaling modulates beta cell apoptosis. J Biol Chem 278:471–478.

Marsden CD. 1990. Parkinson's disease. Lancet 335:948–952.

Merchenthaler I, Lane M, Shughrue P. 1999. Distribution of pre-proglucagon and glucagon-like peptide-1 receptor messenger RNAs in the rat central nervous system. J Comp Neurol 403:261–280.

Meshi D, Drew MR, Saxe M, Ansorge MS, David D, Santarelli L, Malapani C, Moore H, Hen R. 2006. Hippocampal neurogenesis is not required for behavioral effects of environmental enrichment. Nat Neurosci 9:729–731.

Miller GW, Erickson JD, Perez JT, Penland SN, Mash DC, Rye DB, Levey AI. 1999. Immunochemical analysis of vesicular monoamine transporter (VMAT2) protein in Parkinson's disease. Exp Neurol 156:138–148.

Mohapel P, Frielingsdorf H, Haggblad J, Zachrisson O, Brundin P. 2005. Platelet-derived growth factor (PDGF-BB) and brain-derived neurotrophic factor (BDNF) induce striatal neurogenesis in adult rats with 6-hydroxydopamine lesions. Neuroscience 132:767–776.

Montrose-Rafizadeh C, Yang H, Rodgers BD, Beday A, Pritchette LA, Eng J. 1997a. High potency antagonists of the pancreatic glucagon-like peptide-1 receptor. J Biol Chem 272:21201–21206.

Montrose-Rafizadeh C, Yang H, Wang Y, Roth J, Montrose MH, Adams LG. 1997b. Novel signal transduction and peptide specificity of glucagon-like peptide receptor in 3T3-L1 adipocytes. J Cell Physiol 172:275–283.

Nakatomi H, Kuriu T, Okabe S, Yamamoto S, Hatano O, Kawahara N, Tamura A, Kirino T, Nakafuku M. 2002. Regeneration of hippocampal pyramidal neurons after ischemic brain injury by recruitment of endogenous neural progenitors. Cell 110:429–441.

Nygren J, Wieloch T, Pesic J, Brundin P, Deierborg T. 2006. Enriched environment attenuates cell genesis in subventricular zone after focal ischemia in mice and decreases migration of newborn cells to the striatum. Stroke 37:2824–2829.

Parkes DG, Pittner R, Jodka C, Smith P, Young A. 2001. Insulinotropic actions of exendin-4 and glucagon-like peptide-1 in vivo and in vitro. Metabolism 50:583–589.

Perry T, Lahiri DK, Chen D, Zhou J, Shaw KT, Egan JM, Greig NH. 2002. A novel neurotrophic property of glucagon-like peptide 1: a promoter of nerve growth factor-mediated differentiation in PC12 cells. J Pharmacol Exp Ther 300:958–966.

Perry T, Lahiri DK, Sambamurti K, Chen D, Mattson MP, Egan JM, Greig NH. 2003. Glucagon-like peptide-1 decreases endogenous amyloid-beta peptide (Abeta) levels and protects hippocampal neurons from death induced by Abeta and iron. J Neurosci Res 72:603–612.

Saxe M, Malleret G, Vronskaya S, Drew M, Santarelli L, Kandel ER, Hen R. 2006.Paradoxical consequences of ablating hippocampal neurogenesis. Poster 226.6/FF25 14–18 October, Atlanta, GA.

Scharfman HE, Hen R. 2007. Neuroscience. Is more neurogenesis always better? Science 315:336–338.

Schneider A, Kruger C, Steigleder T, Weber D, Pitzer C, Laage R, Aronowski J, Maurer MH, Gassler N, Mier W, Hasselblatt M, Kollmar R, Schwab S, Sommer C, Bach A, Kuhn HG, Schabitz WR. 2005. The hematopoietic factor G-CSF is a neuronal ligand that counteracts programmed cell death and drives neurogenesis. J Clin Invest 115:2083–2098.

Shan X, Chi L, Bishop M, Luo C, Lien L, Zhang Z, Liu R. 2006. Enhanced de novo neurogenesis and dopaminergic neurogenesis in the substantia nigra of 1-methyl-4-phenyl-1,2,3,6-tetrahydropyridine-induced Parkinson's disease-like mice. Stem Cells 24:1280–1287.

Tande D, Hoglinger G, Debeir T, Freundlieb N, Hirsch EC, Francois C. 2006. New striatal dopamine neurons in MPTP-treated macaques result from a phenotypic shift and not neurogenesis. Brain 129:1194–1200.

Taupin P. 2006. Neurogenesis in the adult central nervous system. C R Biol 329:465–475.

Taupin P. 2007. BrdU immunohistochemistry for studying adult neurogenesis: paradigms, pitfalls, limitations, and validation. Brain Res Rev 53:198–214.

Thorens B, Porret A, Buhler L, Deng SP, Morel P, Widmann C. 1993. Cloning and functional expression of the human islet GLP-1 receptor. Demonstration that exendin-4 is an agonist and exendin-(9–39) an antagonist of the receptor. Diabetes 42:1678–1682.

Ungerstedt U, Arbuthnott GW. 1970. Quantitative recording of rotational behavior in rats after 6-hydroxy-dopamine lesions of the nigrostriatal dopamine system. Brain Res 24:485–493.

Van Kampen JM, Eckman CB. 2006. Dopamine D3 receptor agonist delivery to a model of Parkinson's disease restores the nigrostriatal pathway and improves locomotor behavior. J Neurosci 26:7272–7280.

Wheeler MB, Lu M, Dillon JS, Leng XH, Chen C, Boyd AE 3rd. 1993. Functional expression of the rat glucagon-like peptide-I receptor, evidence for coupling to both adenylyl cyclase and phospholipase-C. Endocrinology 133:57–62.

Yamamoto H, Lee CE, Marcus JN, Williams TD, Overton JM, Lopez ME, Hollenberg AN, Baggio L, Saper CB, Drucker DJ, Elmquist JK. 2002. Glucagon-like peptide-1 receptor stimulation increases blood pressure and heart rate and activates autonomic regulatory neurons. J Clin Invest 110:43–52.

Yamamoto H, Kishi T, Lee CE, Choi BJ, Fang H, Hollenberg AN, Drucker DJ, Elmquist JK. 2003. Glucagon-like peptide-1-responsive catecholamine neurons in the area postrema link peripheral glucagon-like peptide-1 with central autonomic control sites. J Neurosci 23:2939–2946.

Yang H, Egan JM, Wang Y, Moyes CD, Roth J, Montrose MH, Montrose-Rafizadeh C. 1998. GLP-1 action in L6 myotubes is via a receptor different from the pancreatic GLP-1 receptor. Am J Physiol 275:C675–C683.

Zhao M, Momma S, Delfani K, Carlen M, Cassidy RM, Johansson CB, Brismar H, Shupliakov O, Frisen J, Janson AM. 2003. Evidence for neurogenesis in the adult mammalian substantia nigra. Proc Natl Acad Sci U S A 100:7925–7930.